

Theoretical and Numerical Study of Symmetric, In-plane, Free Vibration of Timoshenko Portal Frame with Open Crack

Nikam M Satyavan, Sandeep Kumar and S.M. Murigendrappa*

Department of Mechanical Engineering, National Institute of Technology Karnataka, Surathkal-575025, India

*Corresponding author: smm@nitk.ac.in

Abstract The local flexibility introduced by cracks changes the vibration behaviour of the structure and by examining this change, crack severity can be identified. This paper presents the natural frequencies of symmetric, in-plane free-vibrations of Timoshenko portal frame with and without open crack for different boundary conditions. Cracked segment is modelled as two segments connected by a massless torsional spring. Considering appropriate compatibility requirements at the crack section in any one of segments and at the junction of two segments, the characteristic equations are established for corresponding boundary conditions and solved for natural frequencies by numerically. Crack location ranging from 20% to 70% of length of segment and crack size ranging from 20% to 60% of depth have been considered. Results obtained analytically are compared numerically using standard commercially available finite element software. The frame has been modelled by using quadratic quadrilateral shell elements and quarter-point singular elements are employed around the crack-tip. It is observed that as expected, with increase in crack depth the change in frequencies of the frame with and without crack increases. The maximum difference between the analytical and numerical results is 7.09% for all the cases considered, which proves usefulness of the data.

Keywords Timoshenko Portal Frame, Open Crack, Massless Torsional Spring, In-plane Free Vibration, FEM

1. Introduction

The problem of Timoshenko portal frames with defect is of importance in many fields of engineering. Defects are almost unavoidable in such frames and their existences will decrease stiffness, strength and safety. Although, a number of accurate, effective and reliable on-line damage detection methods based on either X-ray, ultrasonic tests etc., are available, their adoption require scanning of the whole length of frame. This process is a very time consuming, labour-intensive and expensive. In view of these limitations there is a need to develop Non-Destructive Testing methods which can detect damages in a component from the measurement of vibration responses, which may be collected from at a single point, or at the most, a few points, on the component.

The most significant vibration parameter applied in damage identification methods is change in natural frequencies of vibrations of structures caused by the crack. Hence, it may be possible to predict the presence of a crack from the measurements of natural frequencies of the damaged component. A wide variety of beam structures modelled by Euler-Bernoulli or Timoshenko beam theory have been considered for crack detection by representing the crack with massless torsional spring[1-9] etc. Experimental results, though not very exhaustive, are also reported.

Most of the studies on frames consider them to be free from defects [10-16]. A few investigators have reported inverse problem of determination of crack details from the natural frequencies or mode shapes (e.g.,[17-19]) for frame modelled by Euler-Bernoulli beam theory. Frames modelled by Timoshenko beam theory with crack have not yet been studied. This paper presents, a method of solving a forward problem i.e., determination of natural frequencies knowing the crack details of symmetric, in-plane vibrations of Timoshenko portal frame with crack. Associated cracked segment in the portal frame is modelled as two segments connected by a massless torsional spring. The characteristic equations are established using boundary conditions, compatibility conditions at

junctions of two segments and continuity conditions at the crack location. These characteristic equations are used to compute the natural frequencies of Timoshenko portal frame by numerically. Finally, these computed natural frequencies are compared with that of natural frequencies obtained from finite element method for fixed-hinged, hinged-hinged and fixed-fixed end conditions.

2. Theoretical formulation

For in-plane free vibration analysis of Portal frame without and with crack, initially a beam with crack has been studied and natural frequencies have been compared with available literature. For the In-plane free vibration analysis of portal frame, transverse and longitudinal motions of each member are taken into consideration. In analytical modelling of frame, Timoshenko beam theory approach is used for analysis of transverse vibration, while axial vibration of rod is considered for analysis of longitudinal vibration of each member.

A portal frame containing a part through-the-thickness edge crack undergoing free transverse vibration, gives rise to a deformation pattern corresponding to natural frequencies. This in turn will change the slope-mode shape, curvature mode shape, etc. The forward problem of determination of natural frequencies knowing the crack details for fixed-hinged, hinged-hinged and fixed-fixed end conditions have been examined. Accuracy obtainable in connection with natural frequencies is compared numerically using commercially available FE tool for different boundary conditions.

2.1. Formulation for portal frame without crack

For a free, in-plane, symmetric transverse and axial motions of each segments in portal frame without any crack is modelled by using Timoshenko beam theory i.e., taking the effects of shear deformation and rotational inertia. Neglecting damping effect, the mode shape equations of each segments are governed by (Fig. 1)[11]

Transverse motion:

$$v_i''''(\eta_i) + (\sigma + \tau) v_i''(\eta_i) - (\alpha - \sigma\tau) v_i(\eta_i) = 0, \quad 0 < \eta_i < \beta_i \quad \text{for } i = 1,2,3 \quad (1)$$

Slope due to bending:

$$\phi_i''''(\eta_i) + (\sigma + \tau) \phi_i''(\eta_i) - (\alpha - \sigma\tau) \phi_i(\eta_i) = 0, \quad 0 < \eta_i < \beta_i \quad \text{for } i = 1,2,3 \quad (2)$$

Longitudinal motion:

$$u_i''(\eta_i) + \gamma^2 v_i(\eta_i) = 0, \quad 0 < \eta_i < \beta_i \quad \text{for } i = 1,2,3 \quad (3)$$

where v_i is transverse displacement, u_i is axial displacement, ϕ_i is the rotation due to bending of the segments, these are function of non-dimensional position, η_i along the length of segment in a particular mode for the segment i , a prime indicates differentiation with respect to η_i and additional parameters given by

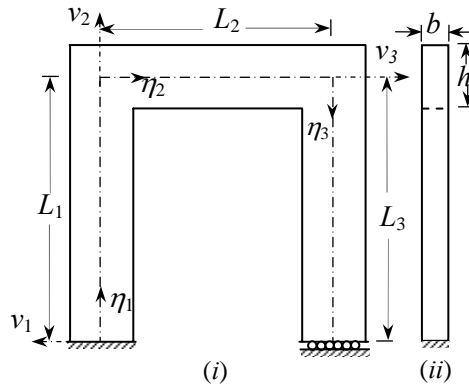


Figure 1. Schematic of Timoshenko portal frame: (i) front view and (ii) side view.

$$\sigma = \frac{\rho L^2 \omega^2}{E}, \tau = \frac{\rho L^2 \omega^2}{\kappa G}, \alpha = \frac{\rho L^4 \omega^2 A}{EI}, \gamma^2 = \frac{\rho L^2 \omega^2}{E}, \beta_i = \frac{L_i}{L}, L = L_1 + L_2 + L_3 \quad (4)$$

E is modulus of elasticity, I is second moment of inertia, A is cross sectional area, G is shear modulus, ρ is density of material, κ is Timoshenko's shear coefficient and its value is 5/6 for rectangular cross-section, L is total length of portal frame.

The solutions of Eq. (1-3) are given by

$$v_i(\eta_i) = A_i \cosh \lambda_1 \eta_i + B_i \sinh \lambda_1 \eta_i + C_i \cos \lambda_2 \eta_i + D_i \sin \lambda_2 \eta_i, \quad 0 < \eta_i < \beta_i \quad \text{for } i = 1, 2, 3 \quad (5)$$

$$\phi_i(\eta_i) = q_1 A_i \sinh \lambda_1 \eta_i + q_1 B_i \cosh \lambda_1 \eta_i + q_2 C_i \sin \lambda_2 \eta_i - q_2 D_i \cos \lambda_2 \eta_i, \quad 0 < \eta_i < \beta_i \quad \text{for } i = 1, 2, 3 \quad (6)$$

$$u_i(\eta_i) = E_i \sin \gamma \eta_i + F_i \cos \gamma \eta_i, \quad 0 < \eta_i < \beta_i \quad \text{for } i = 1, 2, 3 \quad (7)$$

where $\lambda_1 = \sqrt{\left(\frac{\sigma - \tau}{2}\right)^2 + \alpha - \frac{\sigma + \tau}{2}}$, $\lambda_2 = \sqrt{\left(\frac{\sigma - \tau}{2}\right)^2 + \alpha + \frac{\sigma + \tau}{2}}$, $\lambda_3 = \sqrt{\frac{\rho L^2 \omega^2}{\kappa G}}$, $q_1 = \frac{\lambda_1^2 + \lambda_3^2}{\lambda_1}$, $q_2 = \frac{\lambda_3^2 - \lambda_2^2}{\lambda_2}$,

A_i, B_i, C_i, D_i, E_i and F_i are arbitrary constants evaluated from the boundary conditions.

The boundary and compatibility conditions for a fixed-hinged frame (Fig. 1) are as follows.

at $\eta_1 = 0$; $v_1(0) = 0, \phi_1(0) = 0, u_1(0) = 0$ } (8)

at $\eta_3 = \beta_3$; $v_3(\beta_3) = 0, \phi_3'(\beta_3) = 0, u_3(\beta_3) = 0$ }

at $\eta_1 = \beta_1, \eta_2 = 0$; $v_2(0) = u_1(\beta_1), -v_1(\beta_1) = u_2(0), v_2'(0) = v_1'(\beta_1), \phi_2'(0) = \phi_1'(\beta_1)$ } (9)
 $\kappa G[v_2'(0) - \phi_2(0)] = Eu_1'(\beta_1), \kappa G[v_1'(\beta_1) - \phi_1(\beta_1)] = -Eu_2'(0)$ }

at $\eta_2 = \beta_2, \eta_3 = 0$; $v_3(0) = u_2(\beta_2), -v_2(\beta_2) = u_3(0), v_3'(0) = v_2'(\beta_2), \phi_3'(0) = \phi_2'(\beta_2)$ } (10)
 $\kappa G[v_3'(0) - \phi_3(0)] = Eu_2'(\beta_2), \kappa G[v_2'(\beta_2) - \phi_2(\beta_2)] = -Eu_3'(0)$ }

By substituting Eqs. (5-7) in to Eqs. (8-10) results in following 18 homogeneous equations.

$$A_1 + C_1 = 0 \quad (11)$$

$$q_1 B_1 - q_2 D_1 = 0 \quad (12)$$

$$F_1 = 0 \quad (13)$$

$$A_3 \cosh \lambda_1 \beta_3 + B_3 \sinh \lambda_1 \beta_3 + C_3 \cos \lambda_2 \beta_3 + D_3 \sin \lambda_2 \beta_3 = 0 \quad (14)$$

$$A_3 \lambda_1 q_1 \cosh \lambda_1 \beta_3 + B_3 \lambda_1 q_1 \sinh \lambda_1 \beta_3 + C_3 \lambda_2 q_2 \cos \lambda_2 \beta_3 + D_3 \lambda_2 q_2 \sin \lambda_2 \beta_3 = 0 \quad (15)$$

$$E_3 \sin \gamma \beta_3 + F_3 \cos \gamma \beta_3 = 0 \quad (16)$$

$$E_1 \sin \gamma \beta_1 + F_1 \cos \gamma \beta_1 - A_2 - C_2 = 0 \quad (17)$$

$$A_1 \cosh \lambda_1 \beta_1 + B_1 \sinh \lambda_1 \beta_1 + C_1 \cos \lambda_2 \beta_1 + D_1 \sin \lambda_2 \beta_1 + F_2 = 0 \quad (18)$$

$$A_1 \lambda_1 \sinh \lambda_1 \beta_1 + B_1 \lambda_1 \cosh \lambda_1 \beta_1 - C_1 \lambda_2 \sin \lambda_2 \beta_1 + D_1 \lambda_2 \cos \lambda_2 \beta_1 - \lambda_1 B_2 - \lambda_2 D_2 = 0 \quad (19)$$

$$A_1 \lambda_1 q_1 \cosh \lambda_1 \beta_1 + B_1 \lambda_1 q_1 \sinh \lambda_1 \beta_1 + C_1 \lambda_2 q_2 \cos \lambda_2 \beta_1 + D_1 \lambda_2 q_2 \sin \lambda_2 \beta_1 - \lambda_1 q_1 A_2 - \lambda_2 q_2 C_2 = 0 \quad (20)$$

$$\gamma E (E_1 \cos \gamma \beta_1 - F_1 \sin \gamma \beta_1) - \kappa G [B_2 (\lambda_1 - q_1) + D_2 (\lambda_2 + q_2)] = 0 \quad (21)$$

$$\kappa G [A_1 (\lambda_1 - q_1) \sinh \lambda_1 \beta_1 + B_1 (\lambda_1 - q_1) \cosh \lambda_1 \beta_1 - C_1 (\lambda_2 + q_2) \sin \lambda_2 \beta_1 + D_1 (\lambda_2 + q_2) \cos \lambda_2 \beta_1] + E \gamma E_2 = 0 \quad (22)$$

$$E_2 \sin \gamma \beta_2 + F_2 \cos \gamma \beta_2 - A_3 - C_3 = 0 \quad (23)$$

$$A_2 \cosh \lambda_1 \beta_2 + B_2 \sinh \lambda_1 \beta_2 + C_2 \cos \lambda_2 \beta_2 + D_2 \sin \lambda_2 \beta_2 + F_3 = 0 \quad (24)$$

$$A_2 \lambda_1 \sinh \lambda_1 \beta_2 + B_2 \lambda_1 \cosh \lambda_1 \beta_2 - C_2 \lambda_2 \sin \lambda_2 \beta_2 + D_2 \lambda_2 \cos \lambda_2 \beta_2 - \lambda_1 B_3 - \lambda_2 D_3 = 0 \quad (25)$$

$$A_2 \lambda_1 q_1 \cosh \lambda_1 \beta_2 + B_2 \lambda_1 q_1 \sinh \lambda_1 \beta_2 + C_2 \lambda_2 q_2 \cos \lambda_2 \beta_2 + D_2 \lambda_2 q_2 \sin \lambda_2 \beta_2 - \lambda_1 q_1 A_3 - \lambda_2 q_2 C_3 = 0 \quad (26)$$

$$\gamma E (E_2 \cos \gamma \beta_2 - F_2 \sin \gamma \beta_2) - \kappa G [B_3 (\lambda_1 - q_1) + D_3 (\lambda_2 + q_2)] = 0 \quad (27)$$

$$\kappa G [A_2 (\lambda_1 - q_1) \sinh \lambda_1 \beta_2 + B_2 (\lambda_1 - q_1) \cosh \lambda_1 \beta_2 - C_2 (\lambda_2 + q_2) \sin \lambda_2 \beta_2 + D_2 (\lambda_2 + q_2) \cos \lambda_2 \beta_2] + E \gamma E_3 = 0 \quad (28)$$

These can be expressed conveniently in the following form.

$$[\Delta(\omega)]_{8 \times 18} \{C\}_{18 \times 1} = \{0\}_{18 \times 1} \quad (29)$$

where $\{C\} = \{A_1, B_1, \dots, F_3\}^T$ are unknown arbitrary constants.

For non-trivial solution,

$$|\Delta(\omega)| = 0 \quad (30)$$

which gives the characteristic equations. Solving this equation numerically, the natural frequencies of portal frame without crack are obtained.

2.2. Formulation for portal frame with crack located in left vertical segment

One of the convenient methods of modelling the vibration of a beam segment with a crack is to split the segment into two around the crack section and connect them by massless spring element, whose flexibility is given by a matrix of size 6×6 [20,21]. When the various modes of vibration become uncoupled, the size of the flexibility matrix reduces. Particularly, for a pure transverse vibration the matrix is of size 1×1 . That is, there is only one spring element, which is a torsional spring. A typical representation of a portal frame with a crack located in left vertical segment is shown in Fig. 2. The governing mode shape equations of each segment are of the form:

$$v_i''''(\eta_i) + (\sigma + \tau) v_i''(\eta_i) - (\alpha - \sigma\tau) v_i(\eta_i) = 0, \quad 0 < \eta_i < \beta_i \quad \text{for } i = 1, 2, 3, 4 \quad (31)$$

$$\phi_i''''(\eta_i) + (\sigma + \tau) \phi_i''(\eta_i) - (\alpha - \sigma\tau) \phi_i(\eta_i) = 0, \quad 0 < \eta_i < \beta_i \quad \text{for } i = 1, 2, 3, 4 \quad (32)$$

$$u_i''(\eta_i) + \gamma^2 v_i(\eta_i) = 0, \quad 0 < \eta_i < \beta_i \quad \text{for } i = 1, 2, 3, 4 \quad (33)$$

where values of β_i are as follows.

$$\beta_1 = \delta L_1/L, \beta_2 = (1-\delta)L_2/L, \beta_3 = L_3/L, \beta_4 = L_4/L \text{ and crack location, } 0 \leq \delta \leq 1 \quad (34)$$

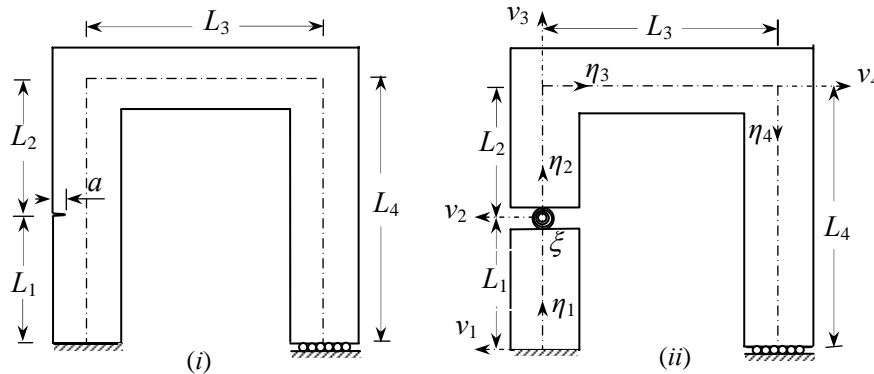


Figure 2. (i) Schematic of Timoshenko portal frame with crack in left vertical segment and (ii) Representation by rotational spring.

The general solutions of Eq. (31-33) are of the form Eqs. (5-7). Boundary and compatibility conditions at the junctions are as follows.

$$\left. \begin{array}{l} \text{at } \eta_1 = 0; \quad v_1(0) = 0, \quad \phi_1(0) = 0, \quad u_1(0) = 0 \\ \text{at } \eta_4 = \beta_4; \quad v_4(\beta_4) = 0, \quad \phi_4'(\beta_4) = 0, \quad u_4(\beta_4) = 0 \end{array} \right\} \quad (35)$$

$$\left. \begin{array}{l} \text{at } \eta_2 = \beta_2, \quad \eta_3 = 0; \quad v_3(0) = u_2(\beta_2), \quad -v_2(\beta_2) = u_3(0), \quad v_3'(0) = v_2'(\beta_2), \quad \phi_3'(0) = \phi_2'(\beta_2) \\ \kappa G[v_3'(0) - \phi_3(0)] = Eu_2'(\beta_2), \quad \kappa G[v_2'(\beta_2) - \phi_2(\beta_2)] = -Eu_3'(0) \end{array} \right\} \quad (36)$$

$$\left. \begin{array}{l} \text{at } \eta_3 = \beta_3, \quad \eta_4 = 0; \quad v_4(0) = u_3(\beta_3), \quad -v_3(\beta_3) = u_4(0), \quad v_4'(0) = v_3'(\beta_3), \quad \phi_4'(0) = \phi_3'(\beta_3) \\ \kappa G[v_4'(0) - \phi_4(0)] = Eu_3'(\beta_3), \quad \kappa G[v_3'(\beta_3) - \phi_2(\beta_3)] = -Eu_4'(0) \end{array} \right\} \quad (37)$$

The compatibility conditions at crack location are given by

$$\left. \begin{array}{l} \text{at } \eta_1 = \beta_1, \quad \eta_2 = 0; \quad v_2(0) = v_1(\beta_1), \quad \phi_2'(0) = \phi_1'(\beta_1), \quad v_2'(0) - \phi_2(0) = v_1'(\beta_1) - \phi_1(\beta_1), \\ v_2''(0) - v_1''(\beta_1) = \xi \phi_1''(\beta_1), \quad u_2(0) = u_1(\beta_1), \quad u_2'(0) = u_1'(\beta_1) \end{array} \right\} \quad (38)$$

where ξ is the non-dimensional flexibility of the torsional spring representing the crack and the relation through crack size can be written in the following form[6]:

$$\xi = 6\pi r^2 \frac{h}{L} f \quad (39)$$

where r is crack size a to segment depth h ratio and f is crack geometry parameter defined by

$$f(r) = 0.6384 - 1.035r + 3.7201r^2 - 5.1773r^3 + 7.533r^4 - 7.332r^5 + 2.4909r^6 \quad (40)$$

By inserting general solutions of type (5-7) into Eqs. (35-38) results in following 24 homogeneous equations.

$$A_1 + C_1 = 0 \quad (41)$$

$$q_1 B_1 - q_2 D_1 = 0 \quad (42)$$

$$F_1 = 0 \quad (43)$$

$$A_4 \cosh \lambda_1 \beta_4 + B_4 \sinh \lambda_1 \beta_4 + C_4 \cos \lambda_2 \beta_4 + D_4 \sin \lambda_2 \beta_4 = 0 \quad (44)$$

$$A_4 \lambda_1 q_1 \cosh \lambda_1 \beta_4 + B_4 \lambda_1 q_1 \sinh \lambda_1 \beta_4 + C_4 \lambda_2 q_2 \cos \lambda_2 \beta_4 + D_4 \lambda_2 q_2 \sin \lambda_2 \beta_4 = 0 \quad (45)$$

$$E_4 \sin \gamma \beta_4 + F_4 \cos \gamma \beta_4 = 0 \quad (46)$$

$$A_1 \cosh \lambda_1 \beta_1 + B_1 \sinh \lambda_1 \beta_1 + C_1 \cos \lambda_2 \beta_1 + D_1 \sin \lambda_2 \beta_1 - A_2 - C_2 = 0 \quad (47)$$

$$A_1 \lambda_1 q_1 \cosh \lambda_1 \beta_1 + B_1 \lambda_1 q_1 \sinh \lambda_1 \beta_1 + C_1 \lambda_2 q_2 \cos \lambda_2 \beta_1 + D_1 \lambda_2 q_2 \sin \lambda_2 \beta_1 - \lambda_1 q_1 A_2 - \lambda_2 q_2 C_2 = 0 \quad (48)$$

$$A_1(\lambda_1 - q_1) \sinh \lambda_1 \beta_1 + B_1(\lambda_1 - q_1) \cosh \lambda_1 \beta_1 - C_1(\lambda_2 + q_2) \sin \lambda_2 \beta_1 + D_1(\lambda_2 + q_2) \cos \lambda_2 \beta_1 - B_2(\lambda_1 - q_1) - D_2(\lambda_2 + q_2) = 0 \quad (49)$$

$$\left. \begin{aligned} & A_1(\lambda_1 \sinh \lambda_1 \beta_1 + \xi \lambda_1 q_1 \cosh \lambda_1 \beta_1) + B_1(\lambda_1 \cosh \lambda_1 \beta_1 + \xi \lambda_1 q_1 \sinh \lambda_1 \beta_1) \\ & + C_1(\xi \lambda_2 q_2 \cos \lambda_2 \beta_1 - \lambda_2 \sin \lambda_2 \beta_1) + D_1(\lambda_2 \cos \lambda_2 \beta_1 + \xi \lambda_2 q_2 \sin \lambda_2 \beta_1) - B_2 \lambda_1 - D_2 \lambda_2 = 0 \end{aligned} \right\} \quad (50)$$

$$E_1 \sin \gamma \beta_1 + F_1 \cos \gamma \beta_1 - F_2 = 0 \quad (51)$$

$$E_1 \cos \gamma \beta_1 - F_1 \sin \gamma \beta_1 - E_2 = 0 \quad (52)$$

$$E_2 \sin \gamma \beta_2 + F_2 \cos \gamma \beta_2 - A_3 - C_3 = 0 \quad (53)$$

$$A_2 \cosh \lambda_1 \beta_2 + B_2 \sinh \lambda_1 \beta_2 + C_2 \cos \lambda_2 \beta_2 + D_2 \sin \lambda_2 \beta_2 + F_3 = 0 \quad (54)$$

$$A_2 \lambda_1 \sinh \lambda_1 \beta_2 + B_2 \lambda_1 \cosh \lambda_1 \beta_2 - C_2 \lambda_2 \sin \lambda_2 \beta_2 + D_2 \lambda_2 \cos \lambda_2 \beta_2 - \lambda_1 B_3 - \lambda_2 D_3 = 0 \quad (55)$$

$$A_2 \lambda_1 q_1 \cosh \lambda_1 \beta_2 + B_2 \lambda_1 q_1 \sinh \lambda_1 \beta_2 + C_2 \lambda_2 q_2 \cos \lambda_2 \beta_2 + D_2 \lambda_2 q_2 \sin \lambda_2 \beta_2 - \lambda_1 q_1 A_3 - \lambda_2 q_2 C_3 = 0 \quad (56)$$

$$\gamma E(E_2 \cos \gamma \beta_2 - F_2 \sin \gamma \beta_2) - \kappa G[B_3(\lambda_1 - q_1) + D_3(\lambda_2 + q_2)] = 0 \quad (57)$$

$$\kappa G[A_2(\lambda_1 - q_1) \sinh \lambda_1 \beta_2 + B_2(\lambda_1 - q_1) \cosh \lambda_1 \beta_2 - C_2(\lambda_2 + q_2) \sin \lambda_2 \beta_2 + D_2(\lambda_2 + q_2) \cos \lambda_2 \beta_2] + E \gamma E_3 = 0 \quad (58)$$

$$E_3 \sin \gamma \beta_3 + F_3 \cos \gamma \beta_3 - A_4 - C_4 = 0 \quad (59)$$

$$A_3 \cosh \lambda_1 \beta_3 + B_3 \sinh \lambda_1 \beta_3 + C_3 \cos \lambda_2 \beta_3 + D_3 \sin \lambda_2 \beta_3 + F_4 = 0 \quad (60)$$

$$A_3 \lambda_1 \sinh \lambda_1 \beta_3 + B_3 \lambda_1 \cosh \lambda_1 \beta_3 - C_3 \lambda_2 \sin \lambda_2 \beta_3 + D_3 \lambda_2 \cos \lambda_2 \beta_3 - \lambda_1 B_4 - \lambda_2 D_4 = 0 \quad (61)$$

$$A_3 \lambda_1 q_1 \cosh \lambda_1 \beta_3 + B_3 \lambda_1 q_1 \sinh \lambda_1 \beta_3 + C_3 \lambda_2 q_2 \cos \lambda_2 \beta_3 + D_3 \lambda_2 q_2 \sin \lambda_2 \beta_3 - \lambda_1 q_1 A_4 - \lambda_2 q_2 C_4 = 0 \quad (62)$$

$$\gamma E(E_3 \cos \gamma \beta_3 - F_3 \sin \gamma \beta_3) - \kappa G[B_4(\lambda_1 - q_1) + D_4(\lambda_2 + q_2)] = 0 \quad (63)$$

$$\kappa G[A_3(\lambda_1 - q_1) \sinh \lambda_1 \beta_3 + B_3(\lambda_1 - q_1) \cosh \lambda_1 \beta_3 - C_3(\lambda_2 + q_2) \sin \lambda_2 \beta_3 + D_3(\lambda_2 + q_2) \cos \lambda_2 \beta_3] + E \gamma E_4 = 0 \quad (64)$$

Eqs. (41-64) can be expressed conveniently in the following matrix equation.

$$[\Delta(\omega, \xi)]_{24 \times 24} \{C\}_{24 \times 1} = \{0\}_{24 \times 1} \quad (65)$$

where $\{C\} = \{A_1, B_1, \dots, F_4\}^T$ are unknown arbitrary constants.

For non-trivial solution

$$|\Delta(\omega, \xi)| = 0 \quad (66)$$

Evaluation of Eq. (66) numerical method yields natural frequencies of portal frame with crack.

2.3. Formulation for Portal frame with crack located in horizontal segment

The modelling of portal frame with crack located in horizontal segment (Fig.3) is done in the similar way as explained in the preceding section. The characteristic equations of type (66) can be obtained by incorporation of the following compatibility conditions at two junctions and crack location with associated boundary conditions.

$$\left. \begin{aligned} \text{at } \eta_1 = \beta_1, \quad \eta_2 = 0; \quad v_2(0) = u_1(\beta_1), \quad -v_1(\beta_1) = u_2(0), \quad v_2'(0) = v_1'(\beta_1), \quad \phi_2'(0) = \phi_1'(\beta_1) \\ \kappa G[v_2'(0) - \phi_2(0)] = E u_1'(\beta_1), \quad \kappa G[v_1'(\beta_1) - \phi_1(\beta_1)] = -E u_2'(0) \end{aligned} \right\} \quad (67)$$

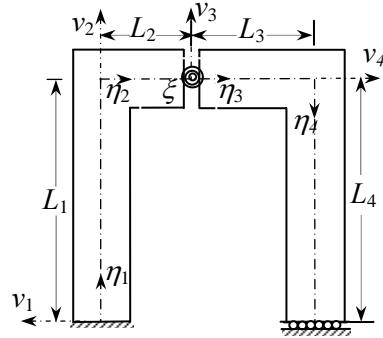


Figure 3. Schematic of Timoshenko portal frame with crack located in horizontal segment represented by torsional spring.

$$\left. \begin{aligned} \text{at } \eta_3 = \beta_3, \quad \eta_4 = 0; \quad v_4(0) = u_3(\beta_3), \quad -v_3(\beta_3) = u_4(0), \quad v_4'(0) = v_3'(\beta_3), \quad \phi_4'(0) = \phi_3'(\beta_3) \\ \kappa G[v_4'(0) - \phi_4(0)] = Eu_3'(\beta_3), \quad \kappa G[v_3'(\beta_3) - \phi_2(\beta_3)] = -Eu_4'(0) \end{aligned} \right\} \quad (68)$$

$$\left. \begin{aligned} \text{at } \eta_2 = \beta_2, \quad \eta_3 = 0; \quad v_3(0) = v_2(\beta_2), \quad \phi_3'(0) = \phi_2'(\beta_2), \quad v_3'(0) - \phi_3(0) = v_2'(\beta_2) - \phi_2(\beta_2), \\ v_3'(0) - v_2'(\beta_2) = \xi \phi_2'(\beta_2), \quad u_3(0) = u_2(\beta_2), \quad u_3'(0) = u_2'(\beta_2) \end{aligned} \right\} \quad (69)$$

For other end conditions; hinged-hinged and fixed-fixed, of portal frame with crack are as follows.

For hinged-hinged ends:

$$\left. \begin{aligned} \text{at } \eta_1 = 0; \quad v_1(0) = 0, \quad \phi_1'(0) = 0, \quad u_1(0) = 0 \\ \text{at } \eta_4 = \beta_4; \quad v_4(\beta_4) = 0, \quad \phi_4'(\beta_4) = 0, \quad u_4(\beta_4) = 0 \end{aligned} \right\} \quad (70)$$

For fixed-fixed ends:

$$\left. \begin{aligned} \text{at } \eta_1 = 0; \quad v_1(0) = 0, \quad \phi_1(0) = 0, \quad u_1(0) = 0 \\ \text{at } \eta_4 = \beta_4; \quad v_4(\beta_4) = 0, \quad \phi_4(\beta_4) = 0, \quad u_4(\beta_4) = 0 \end{aligned} \right\} \quad (71)$$

3. Finite element computation for natural frequencies

The natural frequencies of portal frame with and without crack are computed for a numerical verification of the solution to forward problem by a standard finite element software (i.e., ANSYS-11[22]). A frame is discretized by Eight-node quadrilateral shell elements and quarter-point singular elements employed around the crack-tip is as shown in Fig. 4.

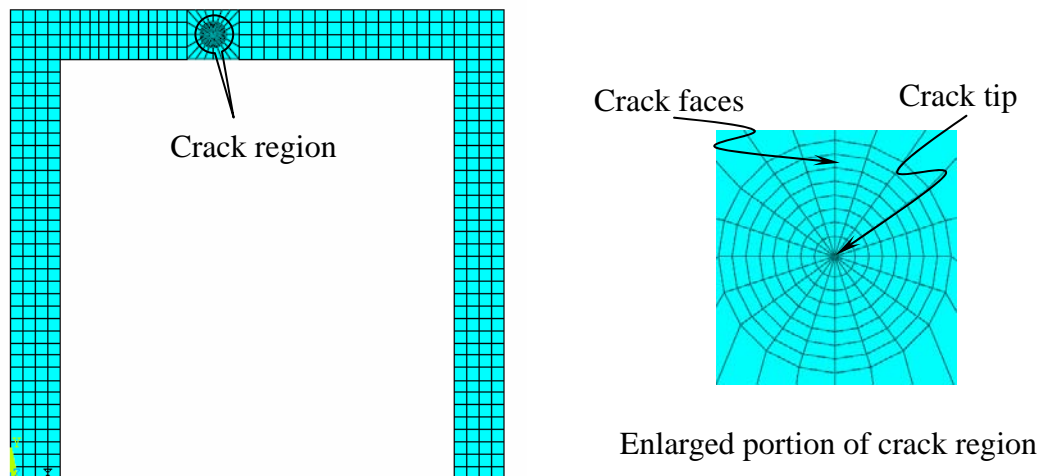


Figure 4. Schematic of finite element modelling of Timoshenko portal frame with crack located in horizontal segment.

4. Results and Discussions

In this study, non-destructive direct solutions for the estimation of the natural frequency of a portal frame with and without crack have been presented. Changes in the natural frequencies of a portal frame due to the presence of a crack may provide additional information for damage detection of these structures. The presence of crack has been theoretically considered by an equivalent torsional spring. To take into account the effects of rotational inertia and shear deformation, Timoshenko beam theory has been employed. The three set of end conditions, fixed-hinged, hinged-hinged and fixed-fixed, have been considered. Crack locations ranging from 20% to 70% of length of segment and crack sizes ranging from 20% to 60% of depth are considered. By means of these boundary conditions and applying suitable compatibility conditions at the cracked section, the characteristic equations have been derived explicitly, whose solution provides the natural frequencies of the portal frame. A MATLAB code has been written to compute the frequencies numerically. The computed natural frequencies have been compared with those obtained by the finite element tool. The geometry of the portal frame with following cross-sectional dimensions and material properties are considered: Length of each no-crack segments (L_i)=0.225m, width (b)=0.0125m and depth (h)=0.025m. The material data employed are: mass density (ρ)= 7800kg/m³, modulus of elasticity $E=210$ GPa, Poisson's ratio $\mu=0.3$ and Timoshenko shear coefficient $\kappa=5/6$. The first three natural frequencies calculated by forward analysis are presented in Tables 1 and 2. The percentage difference in the frequencies taking finite element results as the reference is shown in the Tables 1 and 2. The maximum difference among all results is 7.09% which proves usefulness of proposed method. As expected, the trend of natural frequencies of portal frame with crack, decreases as the crack size increases in comparison with natural frequencies of portal frame without crack (Fig. 5).

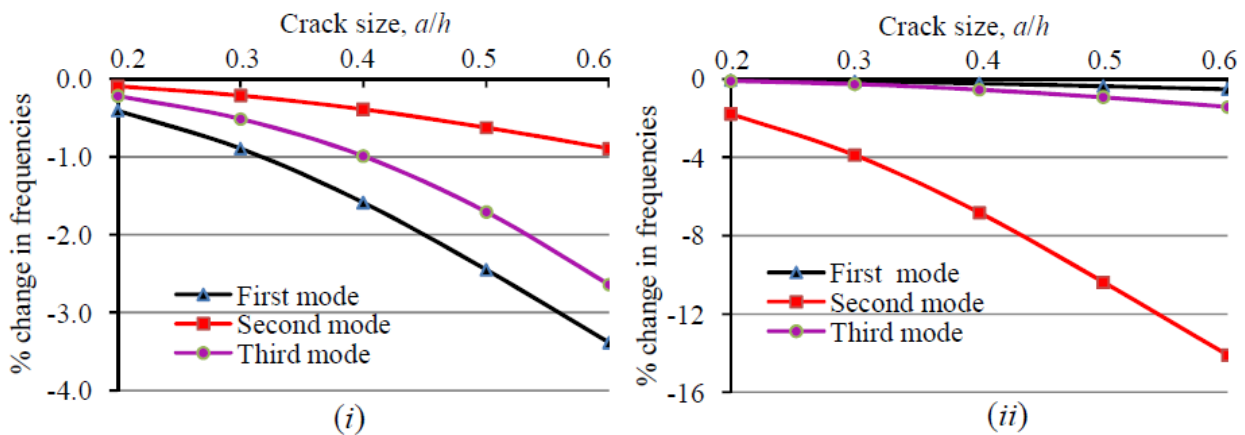


Figure 5. Plot of percentage change in natural frequencies vs. crack size: (i) Fixed-hinged ends of frame with crack located in vertical segment at $\delta=0.4$ and (ii) Fixed-fixed ends of frame with crack located in horizontal segment at $\delta=0.4$.

5. Conclusion

Solution to forward problems i.e. determination of natural frequencies knowing the crack details in Timoshenko portal frame has been studied. The presence of crack has been modelled by an equivalent torsional spring. It is found that the maximum percentage differences between the natural frequencies computed by analytical approach are less than 7.09% as compared to the finite element result. Changes in the natural frequencies of the portal frame due to the presence of a crack may provide additional information for damage detection of these structures.

Table 1. Comparison of natural frequencies computed by analytical method and finite-element method for Timoshenko portal frame with crack located in left vertical segment.

| End cond | Crack loc. δ | a/h | Natural frequencies (Hz) | | | | | | | | | |
|----------|---------------------|---------|--------------------------|------------|------------|-----------------------|------------|------------|--------------|------------|------------|------|
| | | | Analytical method | | | Finite element method | | | % Difference | | | |
| | | | ω_1 | ω_2 | ω_3 | ω_1 | ω_2 | ω_3 | ω_1 | ω_2 | ω_3 | |
| F-H | nocrack | | 278.97 | 1247.63 | 1874.68 | 284.72 | 1253.30 | 1915.70 | 2.02 | 0.45 | 2.14 | |
| | 0.2 | 0.2 | 273.59 | 1246.07 | 1874.27 | 278.67 | 1250.30 | 1914.10 | 1.82 | 0.34 | 2.08 | |
| | | 0.4 | 259.76 | 1242.22 | 1873.25 | 263.04 | 1241.50 | 1909.00 | 1.25 | -0.06 | 1.87 | |
| | | 0.6 | 242.61 | 1237.76 | 1872.06 | 239.40 | 1226.50 | 1898.60 | -1.34 | -0.92 | 1.40 | |
| | 0.4 | 0.2 | 277.82 | 1246.41 | 1870.52 | 283.40 | 1252.70 | 1912.40 | 1.97 | 0.50 | 2.19 | |
| | | 0.4 | 274.53 | 1242.68 | 1855.99 | 279.40 | 1251.40 | 1901.20 | 1.74 | 0.70 | 2.38 | |
| | | 0.6 | 269.52 | 1236.45 | 1825.18 | 271.45 | 1249.70 | 1851.60 | 0.71 | 1.06 | 1.43 | |
| | 0.7 | 0.2 | 278.39 | 1238.80 | 1866.35 | 284.15 | 1245.80 | 1908.50 | 2.03 | 0.56 | 2.21 | |
| | | 0.4 | 276.67 | 1212.19 | 1842.10 | 282.47 | 1225.10 | 1888.50 | 2.05 | 1.05 | 2.46 | |
| | | 0.6 | 273.87 | 1169.33 | 1806.42 | 279.38 | 1186.20 | 1846.20 | 1.97 | 1.42 | 2.15 | |
| | H-H | nocrack | | 171.26 | 1127.17 | 1699.66 | 175.89 | 1127.60 | 1725.90 | 2.63 | 0.04 | 1.52 |
| | | 0.2 | 0.2 | 171.05 | 1121.54 | 1684.13 | 175.73 | 1123.00 | 1707.30 | 2.66 | 0.13 | 1.36 |
| 0.4 | | | 170.33 | 1100.86 | 1631.91 | 175.24 | 1106.70 | 1635.10 | 2.80 | 0.53 | 0.20 | |
| 0.6 | | | 168.74 | 1049.62 | 1536.78 | 174.02 | 1044.30 | 1435.10 | 3.03 | -0.51 | -7.09 | |
| 0.4 | | 0.2 | 170.47 | 1112.51 | 1669.77 | 175.15 | 1114.30 | 1691.40 | 2.67 | 0.16 | 1.28 | |
| | | 0.4 | 167.87 | 1062.04 | 1590.26 | 172.84 | 1068.80 | 1590.50 | 2.88 | 0.63 | 0.02 | |
| | | 0.6 | 162.52 | 963.96 | 1501.23 | 167.14 | 944.69 | 1438.70 | 2.76 | -2.04 | -4.35 | |
| 0.7 | | 0.2 | 169.22 | 1116.83 | 1695.43 | 173.83 | 1118.50 | 1721.50 | 2.65 | 0.15 | 1.51 | |
| | | 0.4 | 162.97 | 1086.81 | 1684.06 | 167.78 | 1093.50 | 1707.90 | 2.87 | 0.61 | 1.40 | |
| | | 0.6 | 152.36 | 1041.43 | 1669.02 | 155.49 | 1047.50 | 1680.50 | 2.01 | 0.58 | 0.68 | |
| F-F | | nocrack | | 371.92 | 1412.93 | 2299.39 | 379.70 | 1426.70 | 2333.60 | 2.05 | 0.97 | 1.47 |
| | | 0.2 | 0.2 | 367.23 | 1411.38 | 2298.55 | 374.29 | 1423.10 | 2332.90 | 1.89 | 0.82 | 1.47 |
| | 0.4 | | 355.35 | 1407.55 | 2296.43 | 360.43 | 1412.50 | 2329.90 | 1.41 | 0.35 | 1.44 | |
| | 0.6 | | 340.98 | 1403.10 | 2293.85 | 339.92 | 1393.40 | 2323.80 | -0.31 | -0.70 | 1.29 | |
| | 0.4 | 0.2 | 371.14 | 1410.18 | 2275.30 | 378.75 | 1425.20 | 2306.00 | 2.01 | 1.05 | 1.33 | |
| | | 0.4 | 368.89 | 1401.69 | 2193.73 | 375.81 | 1421.60 | 2197.10 | 1.84 | 1.40 | 0.15 | |
| | | 0.6 | 365.49 | 1387.23 | 2076.01 | 369.81 | 1415.80 | 1963.20 | 1.17 | 2.02 | -5.75 | |
| | 0.7 | 0.2 | 371.08 | 1399.78 | 2285.05 | 378.86 | 1415.70 | 2318.50 | 2.05 | 1.12 | 1.44 | |
| | | 0.4 | 368.56 | 1361.07 | 2243.52 | 376.45 | 1386.10 | 2286.90 | 2.10 | 1.81 | 1.90 | |
| | | 0.6 | 364.46 | 1301.56 | 2186.91 | 372.01 | 1331.50 | 2155.50 | 2.03 | 2.25 | -1.46 | |

Note: F-H - Fixed-hinged, H-H – Hinged-hinged and F-F – fixed-fixed end conditions.

Table 2. Comparison of natural frequencies computed by analytical method and finite-element method for Timoshenko portal frame with crack located in horizontal segment.

| End cond. | Crack loc. δ | a/h | Natural frequencies (Hz) | | | | | | | | |
|-----------|---------------------|--------|--------------------------|------------|------------|-----------------------|------------|------------|--------------|------------|------------|
| | | | Analytical method | | | Finite element method | | | % Difference | | |
| | | | ω_1 | ω_2 | ω_3 | ω_1 | ω_2 | ω_3 | ω_1 | ω_2 | ω_3 |
| F-H | nocrack | | 278.97 | 1247.63 | 1874.68 | 284.72 | 1253.30 | 1915.70 | 2.02 | 0.45 | 2.14 |
| | 0.2 | 0.2 | 276.55 | 1246.04 | 1865.88 | 282.13 | 1252.10 | 1905.40 | 1.98 | 0.48 | 2.07 |
| | | 0.4 | 269.46 | 1241.25 | 1839.67 | 275.00 | 1248.90 | 1874.90 | 2.01 | 0.61 | 1.88 |
| | | 0.6 | 258.46 | 1233.46 | 1798.69 | 262.03 | 1242.80 | 1816.40 | 1.36 | 0.75 | 0.98 |
| | 0.4 | 0.2 | 278.33 | 1233.51 | 1855.02 | 284.05 | 1240.20 | 1893.60 | 2.01 | 0.54 | 2.04 |
| | | 0.4 | 276.38 | 1190.17 | 1804.91 | 282.21 | 1201.00 | 1834.20 | 2.07 | 0.90 | 1.60 |
| | | 0.6 | 273.01 | 1119.64 | 1746.49 | 278.46 | 1119.40 | 1739.40 | 1.96 | -0.02 | -0.41 |
| | 0.7 | 0.2 | 278.82 | 1231.95 | 1874.48 | 284.52 | 1238.60 | 1915.60 | 2.00 | 0.54 | 2.15 |
| | | 0.4 | 278.37 | 1186.61 | 1873.94 | 283.86 | 1197.80 | 1913.80 | 1.93 | 0.93 | 2.08 |
| 0.6 | | 277.61 | 1118.15 | 1873.15 | 282.40 | 1123.20 | 1908.10 | 1.70 | 0.45 | 1.83 | |
| H-H | nocrack | | 171.26 | 1127.17 | 1699.66 | 175.89 | 1127.60 | 1725.90 | 2.63 | 0.04 | 1.52 |
| | 0.2 | 0.2 | 170.06 | 1121.71 | 1689.28 | 174.53 | 1123.00 | 1714.70 | 2.56 | 0.11 | 1.48 |
| | | 0.4 | 166.48 | 1105.35 | 1660.88 | 170.61 | 1110.50 | 1685.60 | 2.42 | 0.46 | 1.47 |
| | | 0.6 | 160.72 | 1079.11 | 1622.47 | 162.97 | 1087.80 | 1638.10 | 1.38 | 0.80 | 0.95 |
| | 0.4 | 0.2 | 171.12 | 1112.64 | 1698.17 | 175.71 | 1114.20 | 1724.10 | 2.61 | 0.14 | 1.50 |
| | | 0.4 | 170.71 | 1069.01 | 1693.32 | 175.24 | 1075.70 | 1718.60 | 2.59 | 0.62 | 1.47 |
| | | 0.6 | 169.97 | 999.73 | 1684.19 | 174.22 | 999.78 | 1701.00 | 2.44 | 0.01 | 0.99 |
| | 0.7 | 0.2 | 170.72 | 1116.71 | 1694.33 | 175.29 | 1118.20 | 1720.20 | 2.61 | 0.13 | 1.50 |
| | | 0.4 | 169.08 | 1085.34 | 1678.86 | 173.48 | 1091.70 | 1703.30 | 2.54 | 0.58 | 1.43 |
| 0.6 | | 166.31 | 1035.35 | 1655.99 | 169.74 | 1040.60 | 1669.40 | 2.02 | 0.50 | 0.80 | |
| F-F | nocrack | | 371.92 | 1412.93 | 2299.39 | 379.70 | 1426.70 | 2333.60 | 2.05 | 0.97 | 1.47 |
| | 0.2 | 0.2 | 370.06 | 1408.26 | 2284.20 | 377.59 | 1422.60 | 2317.40 | 1.99 | 1.01 | 1.43 |
| | | 0.4 | 364.63 | 1394.43 | 2240.90 | 371.73 | 1410.90 | 2274.90 | 1.91 | 1.17 | 1.49 |
| | | 0.6 | 356.26 | 1372.69 | 2179.08 | 361.01 | 1388.60 | 2202.70 | 1.32 | 1.15 | 1.07 |
| | 0.4 | 0.2 | 371.71 | 1387.86 | 2296.75 | 379.42 | 1402.20 | 2330.50 | 2.03 | 1.02 | 1.45 |
| | | 0.4 | 371.06 | 1316.61 | 2286.83 | 378.70 | 1333.30 | 2318.10 | 2.02 | 1.25 | 1.35 |
| | | 0.6 | 369.92 | 1213.84 | 2266.57 | 377.13 | 1207.20 | 2265.20 | 1.91 | -0.55 | -0.06 |
| | 0.7 | 0.2 | 371.08 | 1397.73 | 2290.78 | 378.77 | 1412.20 | 2324.10 | 2.03 | 1.02 | 1.43 |
| | | 0.4 | 368.54 | 1353.49 | 2265.65 | 376.00 | 1371.00 | 2295.40 | 1.98 | 1.28 | 1.30 |
| 0.6 | | 364.36 | 1286.74 | 2229.64 | 370.48 | 1292.60 | 2234.50 | 1.65 | 0.45 | 0.22 | |

Note: F-H - Fixed-hinged, H-H – Hinged-hinged and F-F – fixed-fixed end conditions.

References

- [1] R.Y. Liang, J. Hu, F.K. Choy, Detection of crack in beam structures using measurement of natural frequencies, *Journal of Franklin Institute*, 328 (1991) 505-518.
- [2] W.M. Ostachowicz, M. Krawczuk, Analysis of the effect of cracks on the natural frequencies of a cantilever beam, *Journal of Sound and vibration*, 150 (1991) 191-201.
- [3] O.S. Salawu, Detection of structural damage through changes in frequency: a review, *Engineering structures*, 19 (1997) 718-723.

- [4] B.P. Nandwana, S.K. Maiti, Detection of location and size of a crack in stepped cantilever beam based on natural frequencies, *Journal of Sound and Vibration*, 203(1997) 435-446.
- [5] S.H.S. Carneiro, D.J. Inman, Continuous model for the transverse vibration of cracked Timoshenko beams, *Transactions of ASME*, 124 (2002) 310-320.
- [6] N. Khaji, M. Shafiei, M. Jalalpour, Closed form solution for crack detection problem of Timoshenko beams with various boundary conditions, *International Journal of Mechanical Science*, 51 (2009) 667-682.
- [7] S.P. Lele and S.K. Maiti, Modelling of transverse vibration of short beams for crack detection and measurement of crack extension, *Journal of Sound and Vibration*, 257 (2002) 559-583.
- [8] J.A. Loya, L. Rubio, J. Fernandez-Saez, Natural frequencies for bending vibration of Timoshenko cracked beams, *Journal of Sound and Vibration*, 290 (2006) 640-653.
- [9] D.Y. Zheng, S.C. Fan, Natural frequency changes of a cracked Timoshenko beam by modified Fourier series, *Journal of Sound and Vibration*, 246 (2001) 297–317.
- [10] C.M. Albarracin, R.O. Grossi, Vibrations of elastically restrained frames, *Journal of Sound and Vibration*, 285 (2005) 467-476.
- [11] H.P. Lin J.D. Wu, Dynamic analysis of planar closed frame structures, *Journal of Sound and Vibration*, 282 (2005) 249-264.
- [12] H.P. Lin, J. Ro, Vibration analysis of planar serial-frame structures, *Journal of Sound and Vibration*, 262 (2003) 1113-1131.
- [13] C.H. Chang, P.Y. Wang, Y.W. Lin, Vibration of X-braced portal frames, *Journal of Sound and Vibration*, 117(1987) 233–248.
- [14] C.P. Filipich, P.A.A. Laura, In-plane vibrations of portal frames with end supports elastically restrained against rotation and translation, *Journal of Sound and Vibration*, 117(1987) 467–474.
- [15] G.M.L. Gladwell, The vibration of frames, *Journal of Sound and Vibration*, 1(1964) 402-425.
- [16] T.M. Wang, T.A. Kinsman, Vibrations of frame structures according to the Timoshenko theory, *Journal of Sound and Vibration*, 14 (1971) 215-227.
- [17] S. Hassiotis, G.D. Jeong, Assessment of structural damage from natural frequency measurement, *Computers and Structures*, 49 (1993) 679-691.
- [18] P.G. Nikolakopoulos, D.E. Katsareas, C.A. Papadopoulos, Crack identification in frame structures, *Computers and Structures*, 64 (1997) 389-406.
- [19] S.M. Murigendrappa, S.K. Maiti, H.R. Srirangarajan, Detection of crack in L-shaped pipes filled with fluid based on transverse natural frequencies, *Structural Engineering and Mechanics-An International Journal*, 21 (2005) 635-658.
- [20] G. Gounaris, A.D. Dimarogonas, A finite element of a cracked prismatic beam for structural analysis, *Computers and Structures*, 28 (1988) 309-313.
- [21] T.G. Chondros, A.D. Dimarogonas, Dynamic sensitivity of structures to cracks, *Transaction of the ASME Journal of Vibration, Acoustics, Stress and Reliability in Design*, 111 (1989) 251-256.
- [22] ANSYS-11.0, User's Manual, 2007.